ELSEVIER

Journal of Organometallic Chemistry 660 (2002) 108–115

Journal of Organometallic Chemistry

www.elsevier.com/locate/jorganchem

Synthesis and evaluation of substituted pyrazoles palladium(II) complexes as ethylene polymerization catalysts

Kelin Li [a], James Darkwa [a,*], Ilia A. Guzei [b], Selwyn F. Mapolie [a]

[a] *Department of Chemistry, University of the Western Cape, Private Bag X17, Bellville 7535, South Africa*
[b] *Department of Chemistry, University of Wisconsin-Madison, Madison, WI 53706, USA*

Received 12 June 2002; received in revised form 29 July 2002; accepted 29 July 2002

Abstract

The substituted pyrazole palladium complexes, (3,5-^{t}Bu$_2$pz)$_2$PdCl$_2$ (**1**) (3,5-Me$_2$pz)$_2$PdCl$_2$ (**2**), (3-Mepz)$_2$PdCl$_2$ (**3**) and (pz)$_2$PdCl$_2$ (**4**) (pzH = pyrazole), can be prepared from the reaction of (COD)PdCl$_2$ with the appropriate pyrazole. The chloromethyl derivative, (3,5-^{t}Bu$_2$pz)$_2$PdCl(Me) (**5**), was prepared from (COD)PdClMe and ^{t}Bu$_2$pzH. X-ray crystal structure determination of **1** and **5** established their structures in the solid state to be the *trans*-isomer. After activation of **1**–**4** and **5** with methylaluminoxane (MAO) the resulting palladium complexes were used as catalysts in ethylene polymerization, yielding linear high-density polyethylene (HDPE). The highest activity was observed for (3,5-^{t}Bu$_2$pz)PdClMe.

Keywords: High density polyethylene (HDPE); Palladium(II); Pyrazole

1. Introduction

Since the first report by Rix and Brookhart that late-transition metal α-diimine complexes dimerize or oligomerize olefins [1], there has been an intensive search for other nitrogen ligand complexes of late-transition metals which can also catalyze olefin oligomerization or polymerization reactions [2]. High molecular weight polyolefins have been reported by Brookhart et al. using palladium(II) and nickel(II) α-diimine complexes [2d]. This has resulted in the exploration of various nitrogen compounds as ligands for late-transition metal complexes, which could be used as catalysts for olefin polymerization. These include bipyridine-type alkene oligomerization catalyst [2d], pyridinylimine ligands [3] and alkylnitrile ligands [4] complexes. Recent patent applications have also reported similar ligand systems in preparing polymerization catalysts [5–7]. In spite of numerous reports on nitrogen ligand complexes of palladium(II) and nickel(II), very little is known about pyrazole and pyrazolyl late-transition metal complexes as catalysts for olefin polymerization. Pyrazoles and their derivatives are attractive ligands as their steric and electronic properties can be fine-tuned by the appropriate choice of substituents on the 2-N, 3-C, 4-C, and 5-C atoms of the pyrazole. This enables the researcher to optimize the electrophilic property of the metal center in an olefin polymerization catalyst.

A report by Jordan et al. on the polymerization of ethylene by [R$_2$C(3-^{t}Bu$_2$pz)$_2$]PdCl$_2$ (R = Me, Ph) [8] is one of the few examples that involve the use of a pyrazolyl ligand, though pyrazole [9] and pyrazolyl [10] ligand–metal compounds abound in the literature. We have recently embarked on a program that involves the use of pyrazole and pyrazolyl compounds as ligands for complexes that could catalyze olefin and acetylene polymerization. The current report presents results of our studies of pyrazole adduct of Pd(II) complexes as olefin polymerization catalysts.

2. Experimental

2.1. Materials and instrumentation

All solvents were analytical grade and used as received except toluene, which was dried over sodium-benzophenone, distilled and stored under a nitrogen atmosphere.

* Corresponding author
E-mail address: jdarkwa@uwc.ac.za (J. Darkwa).

0022-328X/02/$ - see front matter
PII: S0022-328X(02)01799-0

Ethylene (99.9%) was purchased from AFROX (South Africa) and used as received. Methylaluminoxane (MAO) (10 wt.%) in toluene was purchased from Aldrich and transferred in a glove box. The starting materials 3,5-di-*tert*-butylpyrazole [11], (COD)$PdCl_2$ [12] and (COD)PdClMe [13] were synthesized according to literature procedures. All manipulations of air- and/or moisture-sensitive compounds were performed under a dry, deoxygenated nitrogen atmosphere using standard high vacuum or Schlenk techniques. High-pressure polymerization reactions were performed in a mechanically stirred 300 ml Parr autoclave.

IR spectra were recorded as KBr pellets on a Perkin–Elmer, Paragon 1000 PC FTIR spectrometer. NMR spectra were recorded on a Gemini 2000 instrument (^{1}H at 200 MHz, ^{13}C at 50 MHz). Chemical shifts are reported in (ppm) referenced to residual protons and ^{13}C signals of deuterated chloroform as internal reference. ^{13}C-NMR spectra of polyethylene were recorded in 1,2,4-trichlorobenzene at 115 °C. The number- and weight-average molecular weights (M_n and M_w) and polydispersity (M_w/M_n) of polymers were determined by high temperature gel permeation chromatography (GPC) (trichlorobenzene, 145 °C, rate = 1.000 ml min^{-1}). Thermal analyses were performed on a Universal V2.3H TA or a Waters 2000 instrument. Elemental analysis was performed in-house at the department of chemistry, University of the Western Cape. High temperature GPC was performed at the Group Technologies Research and Development laboratory of SASOL Polymers.

2.2. (3,5-^{t}Bu$_2$pz)$_2$PdCl$_2$ (**1**)

To a solution of 3,5-di-*tert*-butylpyrazole (0.58 g, 3.22 mmol) in 40 ml toluene, was added (COD)$PdCl_2$ (0.46 g, 1.61 mmol). The mixture was refluxed until a homogeneous solution was formed. The solvent was evaporated to give a yellow residue, which was recrystallized, from CH_2Cl_2–hexane to afford reddish yellow crystals suitable for X-ray analysis. Yield: 0.53 g (61.3%). ^{1}H-NMR ($CDCl_3$): δ 11.68 (br s, 2H, pyrazole N–H); 5.84 (d, 2H, $^3J_{HH}$ = 2.40 Hz, 4-Pz); 1.78 (s, 18H, 5-^{t}Bu); 1.02 (s, 18H, 3-^{t}Bu). IR (KBr): ν_{N-H} = 3224 cm^{-1}, $\nu_{C=N}$ = 1567 cm^{-1}. Anal. Calc. for $C_{22}H_{40}N_4PdCl_2$: C, 49.12; H, 7.50; N, 10.42. Found: C, 49.40; H, 7.31; N, 10.15%.

2.3. (3,5-Me$_2$pz)$_2$PdCl$_2$ (**2**)

The procedure is the same as for (3,5-^{t}Bu$_2$pz)$_2$$PdCl_2$. Yield: 75.4%. ^{1}H-NMR ($CDCl_3$): δ 11.84 (br s, 2H, N–H); 5.70 (d, 2H, $^3J_{HH}$ = 2.20 Hz, 4-Pz); 2.67 (s, 6H, 5-Me); 1.92 (s, 6H, 3-Me). IR (KBr): ν_{N-H} = 3201 cm^{-1}, $\nu_{C=N}$ = 1579 cm^{-1}. Anal. Calc. for $C_{10}H_{16}N_4PdCl_2$: C, 32.50; H, 4.36; N, 15.16. Found: C, 33.05; H, 5.11; N, 14.18%.

2.4. (3-Mepz)$_2$PdCl$_2$ (**3**)

The procedure is the same as for (3,5-^{t}Bu$_2$pz)$_2$$PdCl_2$. Yield: 98.3%. ^{1}H-NMR ($CDCl_3$): δ 11.24 (br s, 2H, N–H); 7.90–7.92 (dd, 2H, $^3J_{HH}$ = 3.10 Hz, $^4J_{HH}$ = 1.80 Hz, 5-Pz); 6.05 (br s, 2H, 4-Pz); 2.31 (s, 6H, 3-Me). IR (KBr): ν_{N-H} = 3297 cm^{-1}, $\nu_{C=N}$ = 1561 cm^{-1}. Anal. Calc. for $C_8H_{12}N_4PdCl_2$: C, 28.14; H, 3.54; N, 16.41. Found: C, 29.37; H, 3.10; N, 16.03%.

2.5. (pz)$_2$PdCl$_2$ (**4**)

The procedure is the same as for (3,5-^{t}Bu$_2$pz)$_2$$PdCl_2$. Yield: 95.7%. ^{1}H-NMR ($CDCl_3$): δ 11.69 (br s, 2H, N–H); 8.12–8.14 (m, 2H, 5-Pz); 7.58–7.61 (dd, 2H, $^3J_{HH}$ = 1.90 Hz, $^4J_{HH}$ = 0.80 Hz, 3-Pz); 6.37–6.40 (m, 2H, 4-Pz). IR (KBr): ν_{N-H} = 3303 cm^{-1}, $\nu_{C=N}$ = 1515 cm^{-1}. Anal. Calc. for $C_8H_{12}N_4PdCl_2$: C, 22.99; H, 2.57; N, 17.87. Found: C, 24.74; H, 2.41; N, 17.86%.

2.6. (3,5-^{t}Bu$_2$pz)$_2$PdClMe (**5**)

A solution of 3,5-di-*tert*-butylpyrazole (1.00 g, 5.56 mmol) in diethyl ether (60 ml) was added to a solution of (COD)PdClMe (0.8 g, 2.78 mmol) in diethyl ether (60 ml). A light yellow precipitate was formed after 30 min and the reaction was stirred for a further 2 h. the precipitate was filtered and washed with ether. The yellow solid was recrystallized from CH_2Cl_2 at −15 °C to give yellow crystals suitable for X-ray analysis. Yield: 1.20 g (83.5%). ^{1}H-NMR ($CDCl_3$):δ 12.47 (br s, 2H, N–H); 5.80 (d, 2H, $^3J_{HH}$ = Hz, 4-Pz); 1.67 (s, 18H, 5-^{t}Bu); 0.99 (s, 18H, 3-^{t}Bu); −0.14 (s, 3H, Pd–Me). ^{13}C{^{1}H}-NMR ($CDCl_3$): δ 162.9, 155.1, 100.4, 32.1, 30.9, 30.8, 30.1, −4.7.

2.7. General procedure for polymerization of ethylene with substituted pyrazole Pd(II) complexes as catalyst precursors

Polymerization was carried out in a 300 ml stainless steel autoclave, which was loaded with the catalyst and co-catalyst, MAO, in a nitrogen purged glove box. This was done as follows: the autoclave was charged with a palladium complex in dry toluene (150 ml), and appropriate amount of MAO (10% in toluene) (Al–Pd = 250:1000) was added in glove box. The reactor was sealed and removed from the glove box. The autoclave was flushed three times with ethylene and heated to the polymerization temperature. Ethylene was continuously supplied to maintain constant pressure during the polymerization. After the set experiment time, excess ethylene was vented and the polymerization quenched by adding ethanol. The polymer was filtered, washed with 2 M HCl followed by ethanol. It was dried in an oven overnight at 50 °C under vacuum.

2.8. X-ray structural determination

Crystals of $\mathbf{1}\cdot CH_2Cl_2$, $\mathbf{1}\cdot 1/2Et_2O$ and **5** suitable for X-ray crystallography were grown by layering the CH_2Cl_2 mother liquor with either hexane or ether. Crystals of **1** and **5** suitable for X-ray crystallography were selected under oil at ambient conditions and attached to the tip of a glass capillary. Crystal evaluation and data collection were performed on a Bruker CCD-1000 diffractometer with Mo–K_α ($\lambda = 0.71073$ Å) radiation and the diffractometer to crystal distance of 4.9 cm. The initial cell constants were obtained from three series of ω-scans at different starting angles. The reflections were successfully indexed by an automated indexing routine built in the SMART program. The absorption correction was based on fitting a function to the empirical transmission surface as sampled by multiple equivalent measurements [14]. The structures were solved by direct methods and refined by least-squares techniques using SHELXTL program [15]. All non-hydrogen atoms were refined with anisotropic displacement coefficients. All hydrogen atoms were included in the structure factor calculation at idealized positions and were allowed to ride on the neighboring atoms with relative isotropic displacement coefficients.

In the case of $\mathbf{1}\cdot CH_2Cl_2$, there are two symmetry independent molecules of the complex in the asymmetric unit. In each molecule one *tert*-butyl group is disordered over two positions. In the Pd(1) molecule the disorder ratio is 60:40, while in the Pd(2) molecule the ratio is 50:50. There are also two molecules of solvate dichloromethane in the asymmetric unit. In the case of $\mathbf{1}\cdot 1/2Et_2O$, the asymmetric unit contains two symmetry independent molecules of the complex and one solvate molecule of diethyl ether. In one molecule, the *tert*-butyl group at atom C(41) is disordered over two positions in a 72:28 ratio. This disordered group and the *tert*-butyl moiety at C(8) were refined with soft restraints.

3. Results and discussions

3.1. Synthesis

Bis(substituted-pyrazole)palladium(II) chloride complexes were readily prepared according to Scheme 1 from the reaction of four different pyrazole compounds with $(COD)PdCl_2$. The complexes were isolated in moderate to high yields and fully characterized by IR and ^{1}H-NMR spectroscopy as well as by elemental analysis. Complex **1** was further characterized by X-ray crystallography (Fig. 1, Table 2). By a similar route to the above, complex **5** was prepared using (COD)PdClMe in place of $(COD)PdCl_2$. It was similarly characterized by the above analytical techniques, including X-ray crystallography (Table 3). It was essential to prepare **5** in a solvent in which the starting materials are soluble but the product is insoluble. This is due to the instability of **5** in solution at room temperature. In contrast, **1**–**4** was stable in CH_2Cl_2 and toluene over several days without showing any signs of decomposition.

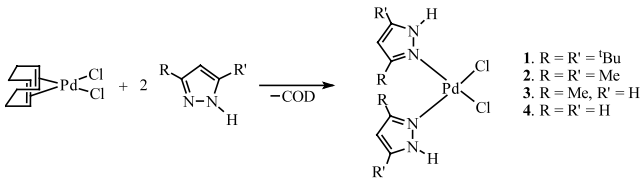

Scheme 1.

3.2. Molecular structures of *1* and *5*

The crystallographic data for $\mathbf{1}\cdot CH_2Cl_2$, $\mathbf{1}\cdot 1/2Et_2O$ and **5** are presented in Table 1. The relevant bond distances and angles are tabulated in Tables 2–4, while the representative molecules of **1** and **5** are shown in Figs. 1 and 2, respectively.

The three palladium complexes share similar structural features. The Pd atom in each complex is in a slightly distorted square-planar environment with the pyrazole ligand *trans* to each other. In all complexes, the pyrazole NH groups are on the same side of the Pd coordination plane. The angles about the central metal range between 85.78(13) and 95.08(8)° while the average Pd–N(pz) distance is calculated to be 2.026(10) Å and fall in the usual range of Pd–N interactions [16].

The Pd–Cl distances in $\mathbf{1}\cdot CH_2Cl_2$ and $\mathbf{1}\cdot 1/2Et_2O$ are different from those in **5** due to different coordination arrangements in the complexes. In the structures of $\mathbf{1}\cdot CH_2Cl_2$ and $\mathbf{1}\cdot 1/2Et_2O$, there is no *trans*-influence among the ligands, but one Pd–Cl bond distance (average 2.286(3) Å) is considerably shorter than the other one (average 2.341(8) Å). This is not surprising since the latter participates in two types of hydrogen bonding interactions that cause the elongation of the Pd–Cl distance. In **5**, the chloride ligands are also

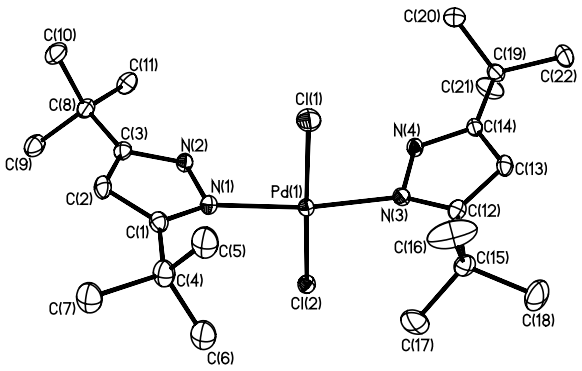

Fig. 1. A molecular drawing of **1** shown with 30% probability ellipsoids. The hydrogen atoms are omitted for clarity.

Table 1
Crystal data and structure refinement for complexes **1** and **5**

	1·CH_2Cl_2	**1**·1/2Et_2O	**5**
Empirical formula	$C_{23}H_{42}Cl_4N_4Pd$	$C_{24}H_{45}Cl_2N_4O_{0.5}Pd$	$C_{23}H_{43}ClN_4Pd$
Formula weight	622.81	574.94	517.46
Temperature (K)	173(2)	173(2)	173(2)
Wavelength (Å)	0.71073	0.71073	0.71073
Crystal system	Triclinic	Triclinic	Monoclinic
Space group	$P\bar{1}$	$P\bar{1}$	$P2_1/n$
a (Å)	13.9501(7)	10.8930(5)	12.8489(11)
b (Å)	15.0175(7)	15.2871(7)	15.5426(13)
c (Å)	15.8089(8)	18.0632(8)	14.0218(12)
α (°)	79.462(1)	92.295(1)	90
β (°)	65.622(1)	107.404(1)	110.059(1)
γ (°)	80.652(1)	92.365(1)	90
V (Å^3)	2951.7(3)	2863.4(2)	2630.4(4)
Z	4	4	4
D_{calc} (Mg m^{-3})	1.401	1.334	1.307
Absorption coefficient (mm^{-1})	1.008	0.854	0.822
$F(000)$	1288	1204	1088
Crystal size (mm^3)	0.40 × 0.40 × 0.40	0.40 × 0.40 × 0.30	0.23 × 0.23 × 0.23
θ Range for data collection (°)	1.39–26.37	1.83–26.38	2.14–26.37
Index ranges	$-15 \le h \le 17$, $-18 \le k \le 18$, $0 \le l \le 19$	$-13 \le h \le 12$, $-19 \le k \le 19$, $0 \le l \le 22$	$-16 \le h \le 15$, $0 \le k \le 19$, $0 \le l \le 17$
Reflections collected	26 299	15 401	16 718
Independent reflections	11 984 [$R_{int} = 0.0242$]	10 957 [$R_{int} = 0.0234$]	5352 [$R_{int} = 0.0434$]
Completeness to $\theta = 26.37°$ (%)	99.2	93.5	99.5
Absorption correction	Empirical with SADABS	Empirical with SADABS	Empirical with SADABS
Max/min transmission	0.6885 and 0.6885	0.7837 and 0.7263	0.8463 and 0.8463
Refinement method	Full-matrix least-squares on F^2	Full-matrix least-squares on F^2	Full-matrix least-squares on F^2
Data/restraints/parameters	11 984/30/605	10 957/18/566	5352/0/276
Goodness-of-fit on F^2	1.056	1.026	1.050
Final R indices [$I > 2\sigma(I)$]	$R_1 = 0.0316$, $wR_2 = 0.0722$	$R_1 = 0.0405$, $wR_2 = 0.1073$	$R_1 = 0.0380$, $wR_2 = 0.0896$
R indices (all data)	$R_1 = 0.0451$, $wR_2 = 0.0760$	$R_1 = 0.0540$, $wR_2 = 0.1146$	$R_1 = 0.0545$, $wR_2 = 0.0966$
Largest difference peak and hole (e Å^{-3})	0.770 and −0.677	1.110 and −1.024	1.380 and −0.809

Table 2
Selected bond lengths (Å) and angles (°) for complex **1**·CH_2Cl_2

Bond lengths			
Pd(1)–N(3)	2.013(2)	Pd(1)–N(1)	2.020(2)
Pd(1)–Cl(1)	2.2822(7)	Pd(1)–Cl(2)	2.3485(7)
N(1)–C(1)	1.345(3)	N(1)–N(2)	1.357(3)
N(3)–C(12)	1.338(3)	N(3)–N(4)	1.361(3)
Pd(2)–N(5)	2.013(2)	Pd(2)–N(7)	2.020(2)
Pd(2)–Cl(3)	2.2866(8)	Pd(2)–Cl(4)	2.3318(7)
N(5)–C(23)	1.342(3)	N(5)–N(6)	1.365(3)
N(7)–C(34)	1.341(3)	N(7)–N(8)	1.363(3)
Bond angles			
N(3)–Pd(1)–N(1)	171.91(9)	N(3)–Pd(1)–Cl(1)	87.13(6)
N(1)–Pd(1)–Cl(1)	88.03(6)	N(3)–Pd(1)–Cl(2)	90.96(6)
N(1)–Pd(1)–Cl(2)	93.47(6)	Cl(1)–Pd(1)–Cl(2)	176.09(3)
C(1)–N(1)–Pd(1)	136.99(18)	N(2)–N(1)–Pd(1)	113.97(16)
C(12)–N(3)–Pd(1)	136.82(18)	N(4)–N(3)–Pd(1)	112.41(16)
N(5)–Pd(2)–N(7)	173.19(9)	N(5)–Pd(2)–Cl(3)	87.53(6)
N(7)–Pd(2)–Cl(3)	87.03(7)	N(5)–Pd(2)–Cl(4)	92.04(6)
N(7)–Pd(2)–Cl(4)	93.06(7)	Cl(3)–Pd(2)–Cl(4)	175.45(3)
C(23)–N(5)–Pd(2)	136.46(18)	N(6)–N(5)–Pd(2)	114.42(16)
C(34)–N(7)–Pd(2)	135.85(19)	N(8)–N(7)–Pd(2)	112.98(15)

involved in hydrogen bonding and coupled with *trans*-influence of the opposite ligand, the Pd–Cl bond separation is even greater averaging to 2.506(16) Å. While the three types of Pd–Cl bonds observed in the three structures are diverse and the difference is statistically significant, they are in the expected span of the terminal Pd–Cl interaction [17–19]. The aforementioned hydrogen bonding was also anticipated a

Table 3
Bond lengths (Å) and angles (°) for **1**·1/2Et_2O

Bond lengths			
Pd(1)–N(3)	2.024(3)	Pd(2)–N(5)	2.019(3)
Pd(1)–N(1)	2.024(3)	Pd(2)–N(7)	2.019(3)
Pd(1)–Cl(1)	2.2895(9)	Pd(2)–Cl(4)	2.2854(10)
		Pd(2)–Cl(3)	2.3462(9)
Bond angles			
N(3)–Pd(1)–N(1)	170.35(11)	N(5)–Pd(2)–N(7)	172.12(11)
N(3)–Pd(1)–Cl(1)	88.80(8)	N(5)–Pd(2)–Cl(4)	87.72(9)
N(1)–Pd(1)–Cl(1)	87.06(8)	N(7)–Pd(2)–Cl(4)	87.11(9)
N(3)–Pd(1)–Cl(2)	91.54(8)	N(5)–Pd(2)–Cl(3)	92.27(9)
N(1)–Pd(1)–Cl(2)	92.40(8)	N(7)–Pd(2)–Cl(3)	92.53(9)
Cl(1)–Pd(1)–Cl(2)	178.60(3)	Cl(4)–Pd(2)–Cl(3)	176.57(4)

Table 4
Selected bond lengths (Å) and angles (°) for complex **5**

Bond lengths			
Pd–C(1)	2.027(3)	Pd–N(1)	2.035(3)
Pd–N(3)	2.041(3)	Pd–Cl	2.5165(9)
N(1)–C(6)	1.340(4)	N(1)–N(2)	1.364(3)
N(3)–C(17)	1.340(4)	N(3)–N(4)	1.363(3)
Bond angles			
C(1)–Pd–N(1)	86.08(13)	C(1)–Pd–N(3)	85.78(13)
N(1)–Pd–N(3)	170.15(10)	C(1)–Pd–Cl	174.72(11)
N(1)–Pd–Cl	92.53(8)	N(3)–Pd–Cl	95.08(8)
C(6)–N(1)–N(2)	106.1(3)	C(6)–N(1)–Pd	138.1(2)
N(2)–N(1)–Pd	113.14(19)	C(17)–N(3)–N(4)	105.7(3)
C(17)–N(3)–Pd	137.6(2)	N(4)–N(3)–Pd	113.99(18)

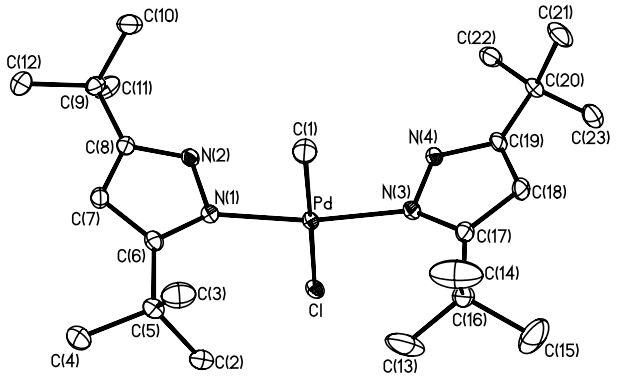

Fig. 2. A molecular drawing of **5** shown with 30% probability ellipsoids. The hydrogen atoms are omitted for clarity.

priori as the pz ligands were expected to retain their 1-H hydrogen atoms which, in turn were to interact with the Cl ligands. Each Cl atom participating in hydrogen bonding forms one inter- and one intra-molecular hydrogen bond.

3.3. Polymerization of ethylene

We conducted a preliminary investigation into the suitability of these substituted pyrazole palladium complexes as catalyst precursors for ethylene polymerization. The main catalyst precursor for most of the ethylene polymerization experiments conducted was $(3,5\text{-}^{t}Bu_2pz)_2PdCl_2$. The results of the polymerization using different catalyst precursors under varying conditions of temperature, ethylene pressure, catalyst precursor concentrations and Al–Pd ratio are listed in Table 5. Catalyst concentration was found to have a pronounced affect on the efficiency of the polymerization process. It was found that catalytic activity dropped when the polymerization is performed at concentrations higher than 4.2×10^{-6} M. This is most likely due to diffusion effects as well as to deactivation via agglomeration of catalyst particles at the higher concentrations. It also appears that at higher catalyst concentration, a lower Al–Pd ratio is more effective. Thus for example slightly higher activity was obtained using an Al–Pd ratio of 250:1 as opposed to 1000:1 when operating at the higher palladium concentration of 12.5×10^{-6} M. At lower palladium concentrations, optimal activity is achieved when an Al–Pd ratio of 1000:1 is employed.

As expected temperature has a marked effect on the polymerization activity. For example the activity is almost doubled when the temperature is raised from 30 to 70 °C. However, the molecular weight of the polymer produced at higher temperature is considerable lower than that produced at 30 °C (entries 4 and 5, Table 5). This is probably due to an increase in the rates of chain transfer and chain termination processes at the higher temperature.

Pressure also affected the polymerization process. Attempts to carry out the reactions at lower pressures than 5 atm did not result in any polymer formation. In some cases only oily–waxy materials were isolated. These are presumably oligomers of ethylene. We are currently investigating reactions at higher pressures.

Of the catalyst precursors evaluated, $(3,5\text{-}^{t}Bu_2pz)_2Pd(Me)Cl$, (**5**) showed the highest activity. A most probable explanation is that this species already has a Pd–Me bond, while all the other precursors are dichlorides. In the case of the latter complexes, MAO would first have to alkylate the Pd–Cl bonds before the active cationic species is formed. This is not the case with the palladium methyl complex, **5**. The overall order of catalyst activity for the different catalyst precursors is **5** > **2** > **4** > **3** > **1**.

From our preliminary results it also appear that longer reaction times also have a detrimental effect on catalyst reactivity. Catalyst precursor **1** for example, deactivation seems relatively rapid with activity being optimal during the first half hour of reaction, after which polymer production fall off to about half its original value after 3 h of reaction time. The deactivation could be related to the relative instability of the activated species in solution.

The polymers produced were characterized by diffuse reflectance Fourier transform infrared spectroscopy (DRIFTS), high temperature ^{13}C-NMR as well as high temperature GPC. The infrared spectra clearly showed saturated alkane peaks at 2929, 2853, 1473, 1463, 1367, and 1349 cm^{-1}. Other peaks observed at 730 and 719 cm^{-1} are associated with long chain alkanes and suggest no branching in the polymer. Further support for only linear polymers was found from ^{13}C-NMR (only one peak at 33 ppm), which also showed the polymer is an ultra-high-molecular-weight polyethylene (UHMWPE) [20]. Molecular weights of selected samples were determined using high temperature GPC and are listed in Table 5. A high average molecular weight, ca. 5.53×10^5 and low polydispersity polymer was obtained when the catalyst precursor **1** or **2** was used. Our observation is

Table 5
Effect of different reaction conditions on the ethylene polymerization

Experiment	Cat	Reaction conditions					TON (kg mol^{-1} h^{-1})	Melting point (°C) (DSC)	M_n ($\times 10^5$)	M_w ($\times 10^5$)	M_w/M_n
		[Pd] (mol l^{-1}) ($\times 10^{-6}$)	Al–Pd ratio	Temperature (°C)	Pressure (atm)	Time (h)					
1	**1**	12.5	1000	25	5	3	174.7	137.07	4.49	5.18	1.15
2	**2**	12.5	500	25	5	3	214.4	145.01	4.67	5.53	1.19
3	**1**	12.5	250	25	5	3	197.5	145.79	4.58	9.65	2.10
4	**1**	4.2	1000	70	5	2.3	1034.5	133.65	1.57	2.78	1.76
5	**1**	4.2	1000	25	5	3	503.0	137.02	5.53	11.89	2.15
6	**1**	4.2	1000	30	5	0.5	1005.7	138.81	5.09	10.24	2.01
7	**2**	4.2	1000	30	5	0.5	1234.9	136.87	4.42	9.43	2.13
8	**3**	4.2	1000	30	5	0.5	1108.6	137.84	4.48	9.23	2.06
9	**4**	4.2	1000	30	5	0.5	1131.9	136.87	4.96	9.94	2.01
10	**5**	4.2	1000	30	5	0.5	1768.1	138.25	5.08	10.15	2.00

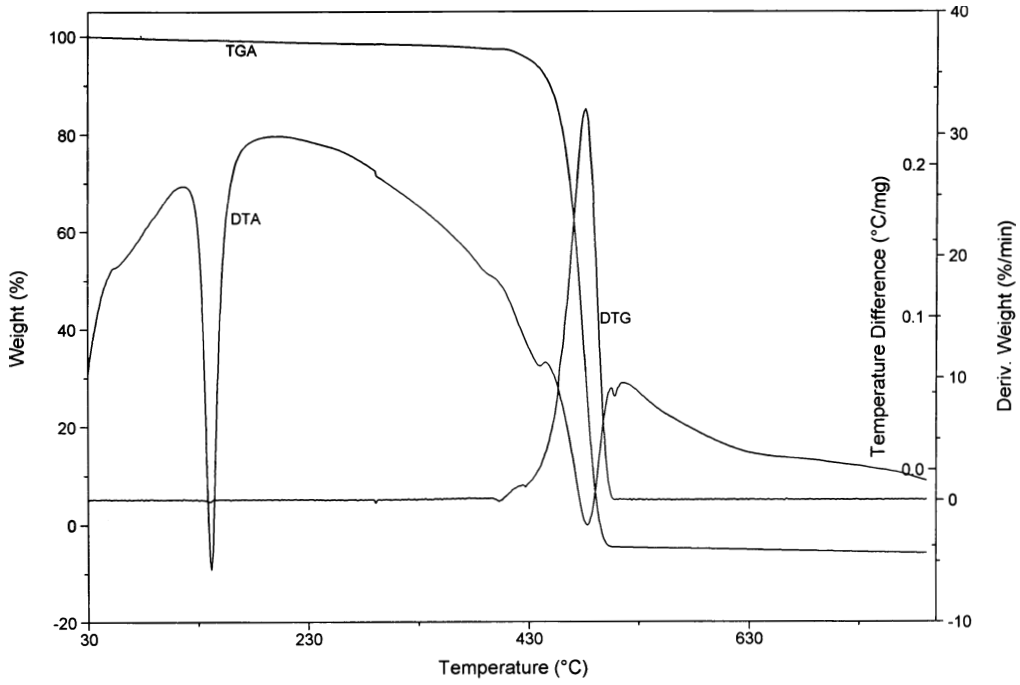

Fig. 3. TGA and DTA of a polyethylene sample.

that at low pressures, low molecular weight polymer with small polydispersity indices was isolated.

To gain insight into the thermal properties of the polyethylene produced in these reactions, we characterized the polymers by differential scanning calorimetry (DSC) as well as thermogravimetric analysis–differential thermal analysis (TGA–DTA). A TGA–DTA thermogram of a polymer (Fig. 3) represents the decomposition of a typical polyethylene [21], which generally occurred from 446 to 500 °C. DSC data of selected polyethylene isolated in this study, together with polymerization conditions are also listed in Table 5. The polymers were found to exhibit melt transition temperatures (T_m) between 132 and 146 °C, which is typical of high-density polyethylene (HDPE). Increasing Al–Pd ratio or temperature gave lower T_m polymers.

4. Conclusions

Four simple pyrazoles have been used to synthesize dichloropalladium and chloromethylpalladium complexes. The chloromethylpalladium complexes are unstable in solution and decomposed within 24 h. All four complexes catalyze the polymerization of ethylene to polyethylene. The structure of the catalyst in solution has a strong effect of the ability of these complexes to polymerize ethylene; with *cis*-isomer being the preferred one. High pressure, high temperature and high co-catalyst to catalyst ratio all increase polymerization. The formation of high density linear polyethylene is confirmed by the results of NMR, DRIFTS and thermal analysis experiments.

Acknowledgements

This work was supported by National Research Foundation (South Africa). We thank SASOL Polymers for the high temperature PGC data.

References

[1] F. Rix, M. Brookhart, J. Am. Chem. Soc. 117 (1995) 1137.
[2] (a) K.A. Ostoja Starzewski, J. Witte, Angew. Chem. Int. Ed. Engl. 26 (1987) 63;
(b) C.M. Killian, L.K. Johnson, M. Brookhart, Organometallics 16 (1997) 2005;
(c) C.M. Killian, D.J. Tempel, L.K. Johnson, M. Brookhart, J. Am. Chem. Soc. 118 (1996) 267;
(d) S.A. Svejda, M. Brookhart, Organometallics 18 (1999) 65.
[3] (a) T.V. Laine, M. Klinga, M. Leskela, Eur. J. Inorg. Chem. (1999) 959;
(b) T.V. Laine, K. Lappalainen, E. Liimatta, B. Aitola, B. Lofgren, M. Lesekela, Macromol. Rapid Commun. 20 (1997) 487;
(c) T.V. Laine, K. Piironen, M. Lappalainen, Klinga, E. Aitola, M. Lesekela, J. Organomet. Chem. 606 (2000) 112;
(d) S.P. Meneghetti, P.J. Lutz, J. Kress, J. Organomet. 18 (1999) 2734.
[4] A. Sen, T. -W. Lai, R.R. Thomas, J. Organomet. Chem. 358 (1988) 567.
[5] P.-L. Bres, V.C. Gibson, C.D.F. Mabille, W. Reed, D. Wass, R.H. Weatherhead, PCT Int. Appl. (1998) 98/49208.
[6] M. Geprags, G. Luinstra, P. Brinkmann, PCT Int. Appl. (1999) 99/03867.

[7] L.K. Johnson, J. Feldman, K.A. Kreutzer, S.J. McLain, A.M.A. Bennett, E.B. Coughlin, D.S. Donald, L.T.J. Nelson, A. Parthasarathy, X. Shen, W. Tam, Y. Wang, PCT Int. Appl. (1997) 97/02298.
[8] S. Tsuji, D.C. Swenson, R.F. Jordan, Organometallics 18 (1999) 4758.
[9] (a) T.G. Schenck, J.W. Downes, C.R.C. Milne, P.B. Mackenzie, H. Boucher, J. Whelan, B. Bosnich, Inorg. Chem. 24 (1985) 2334; (b) A. Satake, T. Nakata, J. Am. Chem. Soc. 120 (1998) 10391; (c) S. Trofimenko, Chem. Rev. 72 (1972) 497.
[10] (a) R.J. Less, J.L.M. Wicks, N.P. Chatterton, M.J. Dewey, N.L. Cromhout, M.A. Halcrow, J.E. Davies, J. Chem. Soc. Dalton Trans. (1996) 4055; (b) K.D. Gallicano, N.L. Paddock, Can. J. Chem. 60 (1982) 521; (c) J.W.F.M. Schoonhoven, W.L. Driessen, J. Reedijk, G.C. Verschoor, J. Chem. Soc. Dalton Trans. (1984) 1053; (d) A. Haskel, E. Keinan, Organometallics 18 (1999) 4677; (e) S. Trofimenko, J. Am. Chem. Soc. 89 (1967) 6288; (f) S. Trofimenko, Chem. Rev. 93 (1993) 943; (g) G. Dong, J.P. Matthews, D.C. Craig, A.T. Baker, Inorg. Chim. Acta 284 (1999) 266; (h) G. Sanchez, J.L. Serrano, J. Perez, M.C.R. Arellano, G. Lopez, E. Molins, Inorg. Chim. Acta 295 (1999) 136.
[11] J. Elguero, E.J.R. Jacquier, Bull. Soc. Chim. Fran. 2 (1968) 707.
[12] D. Drew, J.R. Doyle, Inorg. Synth. 13 (1972) 47.
[13] E. Rule, I.M. Han, C.J. Elsevier, K. Vrieze, P.W.N.M. van Leeuwen, C.F. Roobeek, M.C. Zoutberg, Y.F. Wand, C.H. Stam, Inorg. Chim. Acta 169 (1990) 5.
[14] R.H. Blessing, Acta Crystallogr. Sect. A 51 (1995) 33.
[15] G. Sheldrick, Bruker SHELXTL (Version 5.1), Analytical X-ray Systems, Madison, WI, 1997.
[16] G. Minghetti, M.A. Cinellu, A.B.G. Banditelli, F. Demartin, M. Manassero, J. Organomet. Chem. 15 (1986) 387.
[17] D.B. Grotjahn, D. Combs, S. Van, Inorg. Chem. 39 (2000) 2080.
[18] C.-H. Cheng, J.-S. Lain, Y.-J. Wu, S.-L. Wang, Acta Crystallogr. Sect. C 46 (1990) 208.
[19] B. Douglas, D. McDaniel, J. Alexander, in: Concepts and Models of Inorganic Chemistry, third ed., Wiley, New York.
[20] S.J. Spells, Characterization of solid polymers, in: New Techniques and Developments, Chapman & Hall, London, 1994.
[21] S.R. Sabdler, W. Karo, J. Bonested, E.M. Pearce, Polymer Synthesis and Characterization: A Laboratory Manual, Academic Press, California, 1998.